Performance-Robustness trade-off in the control of a CD player using mixed objectives design

Marco Dettori[1] and Tycho R. Stribos
Mechanical Engineering Systems and Control Group
Delft University of Technology, Mekelweg 2, 2628 CD Delft, The Netherlands.

Abstract

The purpose of this paper is to investigate the possibilities offered by multi-objective control in performing a systematic trade-off between performance and robustness issues in the control design of a CD player. In this control design problem the main goal is to keep the time domain amplitude of a tracking error signal bounded in the presence of disturbances and norm bounded uncertainties. Since these two requirements are conflicting, it is interesting to investigate what are the achievable trade-offs between them. Using the mixed objective approach [1], we construct Pareto optimal curves for this control problem, in correspondence to different choices of norms to represent the specifications. In this way we gain a considerable insight on what is achievable in this design. The resulting controllers are digitally implemented on the real system and validated on the basis of experimental results.

Keywords: Multi-objective control, Linear Matrix Inequalities (LMIs), Pareto optimality, Compact Disc Player.

Notation Due to the lack of a standard notation, we use $\|T\|_{2\to\infty}$ to represent the generalized H_2 norm of the system T. This notation reflects the fact that this norm is the induced gain of the system from L_2 to L_∞.

1 Introduction

It is well-known that classical norm-based control design (e.g. H_∞, H_2, L_1) is not able to handle separate performance/uncertainty channels of the generalized plant in an independent way. All exogenous inputs and performance outputs must be stacked in two vectors and the norm of the overall transfer matrix should be minimized. This can result in a conservative design procedure, since the cross-terms among different channels play an undesirable role in the minimization of the objective function. Furthermore, once the weighting functions have been selected, the trade-off among specifications on different channels is automatically done by the algorithm in a way that cannot be influenced by the designer. To the contrary, multi-objective control techniques allow in principle to treat separate channels in an independent way. The generic multi-objective control problem amounts to the minimization of a certain norm of one channel while the other channels are subject to different norm constraints. Hence, the flexibility of the method clearly results in the free possibility of selecting channels and handling different kinds of norms at the same time. Furthermore, by varying the values of the constraints the designer can achieve different trade-offs without modifying the weighting functions. Unfortunately, so far there are no synthesis algorithms that allow to solve the multi-objective problems in its full generality. In this paper we use the mixed objective approach proposed in [3], [1] that reduces the problem to the solution of an LMI system at the price of introducing an artificial dependence among the different objectives. Our main interest is to investigate to which extent mixed objectives techniques are useful in enlightening the intrinsic relation between performance and robustness in the control problem of the CD player and in allowing to choose the desired compromise among the two requirements. However, the conservatism of the mixed objectives approach can play a role in preventing the assessment of the best trade-off. A sub-goal of this research is, hence, to try to estimate the effects of this conservatism. Finally, this article aims to evaluate the efficiency of the LMI techniques, generally tested on academic examples, in a real control problem and through experimental results.

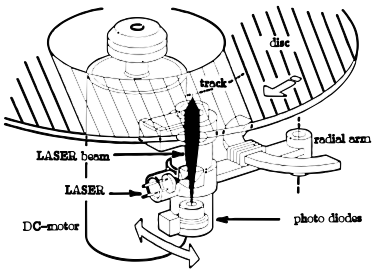

Figure 1: *Schematic view of the CD mechanism*

2 System description and modeling

In figure 1 a schematic view of the CD mechanism is shown. The information to be read is contained in a spiral-shaped track on the surface of a reflective disc, which rotates by effect of a turn-table DC-motor. Track following is performed by a radial arm at the end of which an optical element is mounted. Through a projected laser beam, this optical element retrieves the

[1]Marco Dettori is currently with SC Solutions Inc., Santa Clara, CA, USA. E-mail: dettori@scsolutions.com

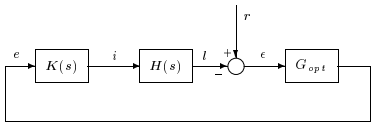

Figure 2: *Block diagram of the CD mechanism*

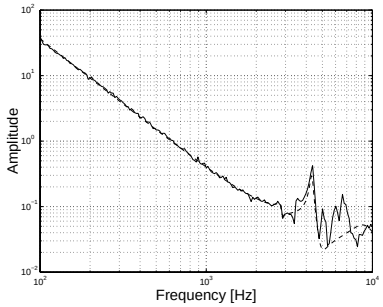

Figure 3: *Measured frequency response (solid line) and fitted model (dashed line)*

information signal together with the position error of the track following. A controller is needed for accurate radial and focus positioning of the projected laser on the track. In this work we consider only the control of the radial positioning, since the LMI design techniques that we use require very long computational times (often longer than 100 hours) to solve the full MIMO problem, which is not manageable when we want to compare several of these designs. On the other hand, the control of the radial positioning is the most challenging in the CD player, since the model of the focus servomechanism is much simpler (see e.g. [4]).

In figure 2 a block diagram of the CD mechanism is shown. $H(s)$ is the transfer function of the mechanical actuator which is controlled by the current i and generates the laser spot l on the disc. G_{opt} is the gain of the optical pick-up mechanism which converts the radial displacement ϵ between track and laser spot in an error signal e. The controller K processes this error signal and generates the current i. The only transfer function that can be identified is the one between i and e, that is $P(s) = -G_{opt}H(s)$. The actual track position r is not measured; we will regard it as an equivalent disturbance signal $d = G_{opt}r$ acting at the output of the plant $P(s)$.

Through closed-loop experiments a frequency response of the plant has been identified. On this data a continuous-time state-space 9^{th} order nominal model has been fitted. For this purpose we used the Matlab toolbox Freqid [7], a graphical user interface to perform curve fitting with user-defined weighting functions. The measured frequency response and the fitted model are shown in figure 3. At low frequencies, the plant behaves like a double integrator, due to the rigid body mode of the radial arm. At higher frequencies, parasitic dynamics appear due to mechanical resonances of the arm construction and to flexible modes of the disc. We chose to model only the first two resonant modes, at about 2.8 and 4.3 kHz, since the others are well beyond the closed-loop relevant frequency range. The main sources of uncertainty we want to account for are the unstructured difference between model and measurements and the variation in the locations of the parasitic resonances. The latter is an effect of manufacturing tolerances in mass production which manifest themselves as variations in the frequency response from player to player. Although this sort of uncertainty can be better described as real parametric, in order to not increase the complexity of the design we will consider it as unstructured norm bounded additive perturbation.

3 Performance specification

The main issue in the control of a CD player is to guarantee a hard bound on the time domain amplitude of the position error signal. To avoid loosing track, the maximum allowable error should be $0.1\mu m$. This bound should be attained in the presence of disturbances. The major disturbance sources are the deviation of the track from the ideal spiral shape and the eccentric rotation of the disc, both related to manufacturing tolerances. As prescribed by the standardization of Compact Discs, the track inaccuracy cannot exceed $100\mu m$. These data imply that a time domain disturbance attenuation of a factor 1000 should be achieved. Due to the geometry of the structure and to the rotating movement, the disturbance signal has predominantly a periodic nature, with fundamental frequency equal to the rotational frequency of the disc. Generally, the approach that is followed to tackle the control problem is to translate the time domain requirement into a frequency domain specification on the shape of the sensitivity function $S = (I + PK)^{-1}$ (see e.g. [5]). Experience showed that, in order to meet the time domain specification for the error, the sensitivity should stay below $-60dB$ up to the highest value of the rotational frequency and should increase to one with a slope possibly not larger than $40dB/dec$. Obviously, this disturbance attenuation requirement puts a lower bound on the achievable closed-loop bandwidth. High bandwidth is undesirable for several reasons: it implies high power consumption (critical especially in portable use), amplification of audible noise and, last but not least, poor robustness against variations in the resonance peaks and unmodeled high frequency dynamics. As a consequence, the wish is for the lowest possible bandwidth, compatibly with the required disturbance suppression. As already mentioned, in the audio application the rotational speed of the disc varies from 4 Hz to 8 HZ, while more advanced applications (like CD-ROM or DVD-ROM) require higher speeds to obtain faster data readout and shorter access time. As a result, the spectrum of the track disturbance is shifted towards higher frequencies, demanding an increase of the bandwidth of the mechanical servosystem in order to achieve the desired suppression. To avoid performance deteriora-

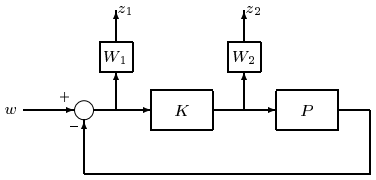

Figure 4: *S/KS control scheme.*

tion due to the resonance peaks, in these applications the quality of the mechanical construction is improved by stiffening the actuators and shifting the parasitic phenomena to higher frequencies. This obviously determines an increase of the manufacturing costs. In this work we want to explore in how far we can guarantee correct operations of the CD mechanism in an increased range of rotational frequencies only through control design, without any plant improvement.

4 Control design

4.1 Single-objective H_∞ design

In this subsection we design a controller for the plant through the use of standard H_∞ minimization. To this end we adopt the so called S/KS control scheme, plotted in figure 4. As already mentioned, the disturbance suppression specification can be imposed by suitably shaping the transfer function of the channel $T_1 : w \to z_1$ with a suitable weighting W_1. The choice

$$W_1(s) = 2\frac{s^2 + 1.2 \cdot 2\pi \cdot 850s + (2\pi \cdot 850)^2}{(s+10)^2((2\pi \cdot 2 \cdot 10^4)^{-1}s + 1)}$$

aims to guarantee a satisfactory disturbance suppression for values of the rotational frequency up to 25 Hz and limits the peak of the Sensitivity by 2. The channel $T_2 : w \to z_2$ admits the interpretation of uncertainty channel. As well known from the small gain theorem, if the closed loop system of figure 4 is nominally stable, then it is also robustly stable against all full-block additive LTI uncertainties Δ such that

$$\|\Delta\|_\infty < \|W_2KS\|_\infty^{-1}.$$

The filter

$$W_2(s) = 0.1\frac{s^2 + 2\pi \cdot 0.6 \cdot 10^3 s + (2\pi \cdot 2 \cdot 10^3)^2}{s^2 + 1.4 \cdot 2\pi \cdot 20 \cdot 10^3 s + (2\pi \cdot 20 \cdot 10^3)^2}$$

represents the behaviour of the uncertainty over frequencies. It has low gain at low frequencies, indicating good system knowledge, and it increases at high frequencies where the knowledge about the system is poorer. These choices for the weighting functions W_1 and W_2 will be used for all the designs in this paper. As a limitation of the standard H_∞ approach, the two channels T_1 and T_2 cannot be handled independently, but they must be grouped in an overall performance channel

$$\begin{pmatrix} z_1 \\ z_2 \end{pmatrix} = \begin{pmatrix} W_1S \\ W_2KS \end{pmatrix} w \qquad (1)$$

whose H_∞ norm has to be minimized. Once the controller has been synthesized, one can compute the obtained values for $\|W_1S\|_\infty$ and $\|W_2KS\|_\infty$ and check what is the compromise between performance and robustness realized by the algorithm. For our design the obtained values are $\|W_1S\|_\infty = 1.34$ and $\|W_2KS\|_\infty = 1.26$.

4.2 H_∞ performance for various levels of robustness

In this subsection we study the problem

$$\begin{aligned} &\inf_{K \text{ stabilizing}} \gamma_p = \|W_1S\|_\infty \\ &\text{subject to } \|W_2KS\|_\infty \le \gamma_r \end{aligned} \qquad (2)$$

for several values of γ_r. This problem has the natural interpretation of finding the best performance level γ_p that can be obtained for different prescribed values of the robustness margin $\frac{1}{\gamma_r}$. We recall that the robustness margin is defined as the norm of the smallest unstructured additive perturbation that destabilizes the closed-loop system. Since we are using two H_∞ norms, problem (2) can be interpreted in loopshaping terms: the bound in the constraint represents the amount of violation of the desired shape of KS that can be tolerated in order to enforce the desired shape for S.

In order to solve problem (2), we apply the mixed objectives techniques of [1]. Due to the conservatism introduced by these techniques we do not obtain the optimal value γ_p, but only an upper bound, which is denoted by $\bar{\gamma}_p$. In the sequel, we will refer to $\bar{\gamma}_p$ as the synthesis value. A lower bound on the difference $\bar{\gamma}_p - \gamma_p$ can be obtained by analysis of the obtained closed-loop system. In fact, if we close the loop with the synthesized mixed objectives controller, the calculated values for $\|W_1S\|_\infty$ and $\|W_2KS\|_\infty$ will be smaller than or equal to $\bar{\gamma}_p$ and γ_r, respectively. As the reason, in the analysis the two norms are calculated independently, without the constraint of a common Lyapunov matrix that is necessary for synthesis (see [1]). Figure 5 shows the trade-off curves for the synthesis and the analysis values of problem (2) that have been obtained for different values of the bound γ_r. The figure shows that the difference between synthesis and analysis values of $\|W_1S\|_\infty$ (along the vertical axis) is pretty small in all the cases and it decreases for increasing values of the constraint γ_r. This does not mean that the method is not conservative, since the curve of the optimal values of problem (2) is unknown. We only know that it should lie below (or, at most, coincide with) the curve of the analysis values. The conservatism can be estimated only through lower bound computations (as suggested in [9]) or the use of Youla techniques to approximate the optimal value [2], [8]). Unfortunately, these techniques are both computationally expensive what makes them not suited for large applications. Figure 5

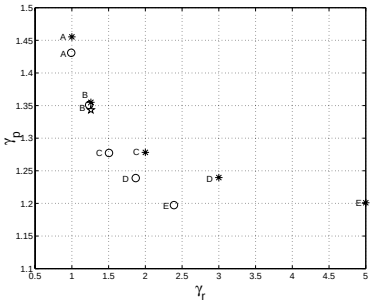

Figure 5: *Trade-off curves for problem (2) for the values $\gamma_r = 1$ (A), $\gamma_r = 1.26$ (B),$\gamma_r = 2$ (C), $\gamma_r = 3$ (D), $\gamma_r = 5$ (E). The stars indicate the synthesis values and the circles the analysis values. The pentagon represents the trade-off achieved by the single-objective H_∞ design.*

also shows that in the cases A and B the analysis value of $\|W_2KS\|_\infty$ is equal to γ_r, meaning that the room left by the constraint is fully used in order to minimize the objective function. In the cases C, D and E, to the contrary, there is an increasing difference between γ_r and the analysis value of $\|W_2KS\|_\infty$. As a possible interpretation, it seems that there is no advantage in further loosening the constraint, since the best performance level allowed by this method has been achieved. Of course, this phenomenon may be just a consequence of the conservatism of the method.

Another interesting observation can be made be comparing the position of the pentagon in figure 5 with the case B. The pentagon represents the values of $\|W_1S\|_\infty$ and $\|W_2KS\|_\infty$ that are obtained by the single-objective S/KS H_∞ design. The case B is the outcome of problem (2) when γ_r is equal to 1.26, the value of $\|W_2KS\|_\infty$ of the single-objective design. The figure shows that the trade-off achieved by the standard H_∞ design lies on the Pareto optimal curve of the mixed objectives method. As a consequence, the mixed objectives design does not allow to obtain better performance for the same robustness level. It is also interesting to notice that the trade-off achieved by the single-objective design lies in a region where synthesis and analysis values for the mixed objectives method are close to each other.

In figures 6 and 7 the behaviors of the S and the KS functions corresponding to the mixed designs are plotted. According to the behavior of the trade-off analysis curve, the shape of the sensitivity function is pushed more towards the inverse of the weighting function for increasing values of γ_r. However, it is also visible that in the region below 1 kHz the Sensitivity tends to a limiting shape and no more suppression can be gained. On the other hand this improvement on the shape of S is counterbalanced by an increase of the amplitude of KS in the region of the plant resonances which causes robustness problems.

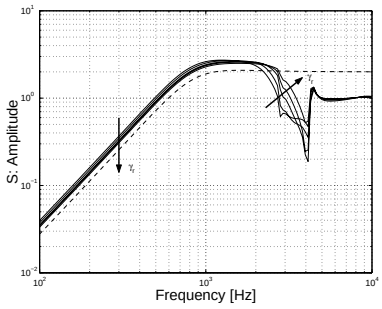

Figure 6: *Behaviors of S for problem (2). The arrows indicate the direction in which γ_r increases. The dashed line is the inverse of the weight W_1.*

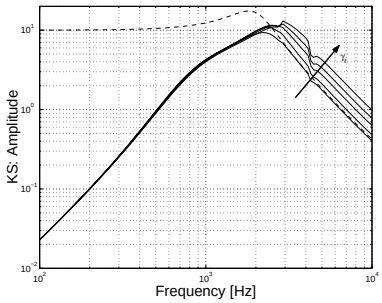

Figure 7: *Behaviors of KS for problem (2). The arrow indicates the direction in which γ_r increases. The dashed line is the inverse of the weight W_2.*

4.3 Generalized H_2 performance for various levels of robustness

In this subsection we analyze a mixed objective problem that admits the same interpretation of the previous one. As the only difference, we use now the generalized H_2 norm to characterize performance. We recall that this norm represents the energy-to-peak gain of the system and, thus, it allows to handle the performance bound for the tracking error directly in the time-domain. The formulation of the problem is

$$\begin{aligned} \inf_{K \text{ stabilizing}} \quad & \gamma_p = \|W_1S\|_{2\to\infty} \\ \text{subject to} \quad & \|W_2KS\|_\infty \le \gamma_r \end{aligned} \tag{3}$$

for several values of γ_r.

The resulting synthesis and analysis trade-off curves are plotted in figure 8. For small values of γ_r, the difference between synthesis and analysis values of $\|W_1S\|_{2\to\infty}$ is rather large. As already observed in the previous case, this difference decreases for increasing γ_r. Again it should be stressed that this does not give any indication about the conservatism of the method. However, it is interesting to note that even in situation A, where the conservatism of the mixed method in the determination of an upper bound of γ_p is quite large, the performance effectively achieved by the designed controller is rather good . Actually, the difference in the achieved performance in all the cases is quite small. As another analogy with the previous problem, the gap

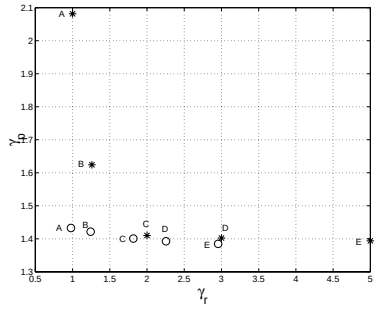

Figure 8: *Trade-off curves for problem (3) for the values $\gamma_r = 1$ (A), $\gamma_r = 1.26$ (B),$\gamma_r = 2$ (C), $\gamma_r = 3$ (D), $\gamma_r = 5$ (E). The stars indicate the synthesis values and the circles the analysis values.*

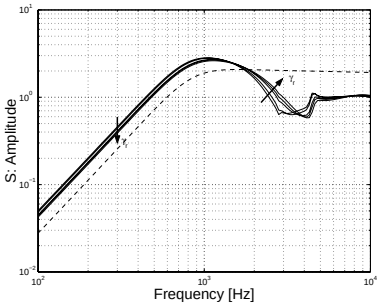

Figure 9: *Behaviors of S for problem (3). The arrows indicate the direction in which γ_r increases. The dashed line is the inverse of the weight W_1.*

between γ_r and the analysis value of $\|W_2KS\|_\infty$ increases with γ_r.

In figures 9 and 10 the behaviors of the S and the KS functions corresponding to these mixed designs are plotted. As a confirmation of the fact that the generalized H_2 norm is not a suitable tool for frequency domain shaping, we observe that the sensitivity function deviates much more from the shape of the inverse of the weight than in the H_∞ case previously treated. Also in the present case, however, the Sensitivity is pushed downwards in the region below 1 kHz for increasing values of γ_r.

In contrast, the behavior of KS is quite different. In fact, the curves stay substantially below the inverse of the weight up to 4.5 kHz, while in the previous case this held only up to 2.5 kHz. This is a favorable aspect, since at higher frequencies our uncertainty model

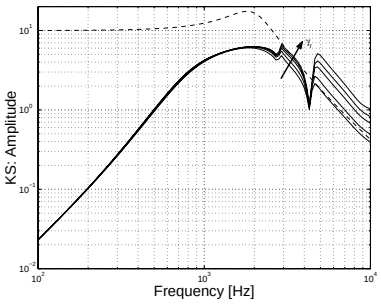

Figure 10: *Behaviors of KS for problem (3). The arrow indicates the direction in which γ_r increases. The dashed line is the inverse of the weight W_2.*

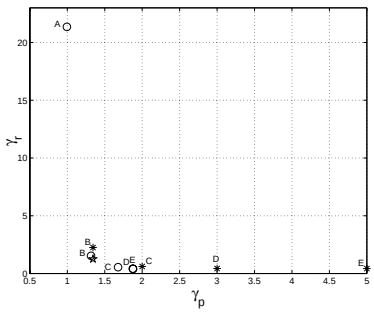

Figure 11: *Trade-off curves for problem (4) for the values $\gamma_p = 1$ (A), $\gamma_p = 1.34$ (B),$\gamma_p = 2$ (C), $\gamma_p = 3$ (D), $\gamma_p = 5$ (E). The stars indicate the synthesis values and the circles the analysis values. The synthesis value in case A is about 600, out of scale. The pentagon represents the trade-off achieved by the single-objective H_∞ S/KS design.*

is very conservative and an increase of KS at 4.5 kHz may have no importance in practice. Figure 10, when compared with figure 7, shows also that the minimization of the generalized H_2 norm of W_1S requires less control effort than the minimization of the corresponding H_∞ norm.

4.4 Achievable robustness for a prescribed performance level

The trade-off between performance and robustness with mixed objectives methods can be analyzed also from a different point of view. Instead of looking what performance can be achieved for different robustness levels, one can think of imposing the desired performance level and determining the achievable robustness margin. This is particularly interesting in view of figure 6, since it seems not possible to push the sensitivity function below the inverse of the weight. A natural question that arises, hence, is whether we are asking a feasible performance specification or, in other words, whether the performance specification represented by W_1 compatible with reasonable robustness properties. Hence, we consider here the mixed problem

$$\inf_{K \text{ stabilizing}} \gamma_r = \|W_2KS\|_\infty \quad \text{subject to} \quad \|W_1S\|_\infty \leq \gamma_p \tag{4}$$

for several values of γ_p. The resulting synthesis and analysis trade-off curves are plotted in figure 11. The most interesting phenomenon is the dramatic decrease of γ_r in passing from the constraint value $\gamma_p = 1$ to the value $\gamma_p = 1.34$, which corresponds to $\|W_1S\|_\infty$ obtained by the single-objective design. When the shape of the sensitivity function is imposed "brute force" to lie below the inverse of the weight, the required control effort blows up destroying the robustness of the design.

5 Implementation results

As explained in section 3, the main goal of our control design is to guarantee correct tracking for increased rotational frequencies. To this end we speeded the velocity of the turn-table motor up to 25 Hz, which is a value

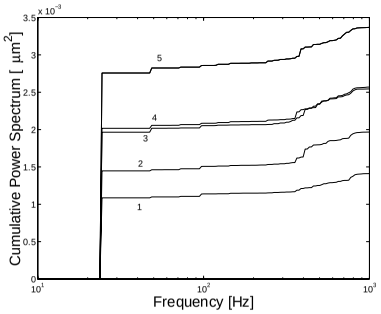

Figure 12: *Cumulative power spectra obtained with several designed controllers.*

about five times bigger than in normal audio applications, by connecting it to an external voltage source. The designed controllers are digitally implemented using a dSpace system that allows also the measurement of the tracking error signal. For more details on the implementation set-up we refer to [6]. A suitable measure to compare the tracking errors achieved by different controllers is the cumulative power spectrum that is the integral of the power spectrum over frequency. Since the tracking error has a periodic behavior, the power spectrum is substantially a series of pulses. The cumulative power spectrum, hence, will exhibit jumps in correspondence to these pulses. The height of each jump is a measure of the power associated to the corresponding harmonic component of the error. In figure 12 the measured cumulative power spectra for several controllers are plotted. Curve 2 corresponds to the single-objective H_∞ design of section 4.1. Curves 1 and 3 correspond to two designs of section 4.2, respectively case C ($\gamma_r = 2$) and case A ($\gamma_r = 1$), where the performance specification was expressed through the H_∞ norm. The experimental results, thus, confirm the trade-off curve of figure 5, where the single-objective design lies between situation A and situation C, and a smaller value of $||W_1 S||_\infty$ results effectively in a smaller tracking error. Unfortunately, the controllers corresponding to cases D and E, with even smaller values of $||W_1 S||_\infty$ turned out to be not implementable, probably due to the excessive size of their control action that saturates the plant actuators. Finally, curves 4 and 5 correspond to the two extreme cases of section 4.3, respectively E ($\gamma_r = 5$) and A ($\gamma_r = 1$), where the performance specification was expressed through the generalized H_2 norm. Also in this case a smaller norm of the performance channel results in a smaller tracking error. However, it clearly appears that the results are worse than in the H_∞ case. This is somewhat surprising, since the generalized H_2 norm is theoretically a better tool than the H_∞ norm to impose time domain amplitude constraints. On the other hand, this outcome can be an effect of the conservatism of the mixed objectives design method that might affect this design much more than the previous one. As a final note, we would have liked to implement also the controller of case A in section 4.4 that would have presumably lead to the best performance but, as to be expected, it turned out not to be implementable.

6 Conclusions

In this paper we have exploited mixed objective control theory in order to derive performance/robustness trade-offs in the design for the tracking servomechanism of a Compact Disc player. The flexibility offered by these techniques allows to derive in a systematic way Pareto optimal curves in correspondence to a large variety of performance criteria and/or robustness measures. The resulting controllers have been validated through real implementation and they succeeded in guaranteeing correct operations of the plant in an increased range of rotational frequencies, as requested by new high-performing applications.

7 Acknowledgements

The authors want to thank Carsten Scherer for his constant support during their research.

References

[1] C. W. Scherer, P. Gahinet and M. Chilali. Multiobjective output-feedback control via LMI optimization. *IEEE Trans. Autom. Control*, 42:896–911, 1997.

[2] H. Hindi, B. Hassibi and S. Boyd. Multiobjective H_2/H_∞ optimal control via a finite dimensional q-parametrization and linear matrix inequalities. In *Proc. Amer. Contr. Conf.*, pages 3244–3248, 1998.

[3] I. Masubuchi, A. Ohara and N. Suda. LMI-based output feedback controller design. In *Proc. American Control Conf.*, pages 3473–3477, 1995.

[4] M. Dettori, V. Prodanovic and C. W. Scherer. Mixed objectives MIMO control design for a compact disc player. In *Proc. Amer. Contr. Conf.*, pages 1284–1288, 1998.

[5] M. Steinbuch, P.J.M. Van Groos, G. Schoostra, P.M. Wortelboer and O.H. Bosgra. μ-synthesis of a compact disc player. *Int. Journ. of Rob. and Nonl. Contr.*, 8:169–189, 1998.

[6] M. Dettori, P. Valk and C.W. Scherer. Digital implementation of a mixed objectives MIMO controller for a compact disc player using a multiprocessor system. In *Proc. American Contr. Conf.*, pages 3630–3634, 1999.

[7] R.A. de Callafon and P.M.J. Van Den Hof. FREQID - Frequency Domain Identification Toolbox for Use with Matlab. In O.H. Bosgra et Al., editor, *Selected Topics in Identification, Modelling and Control.* Delft University Press, 1996.

[8] C.W. Scherer. From mixed to multi-objective control. In *Proc. 38-Th Conf. On Dec. and Contr.*, pages 3621–3626, 1999.

[9] C.W. Scherer. Lower bounds in multi-objectives H_2/H_∞ problems. In *Proc. 38-Th Conf. On Dec. and Contr.*, pages 3605–3610, 1999.